Central peak in the Excitation spectra of thin ferroelectric films

J. M. Wesselinowa*
Department of Physics, University of Sofia, Boulevard J. Bouchier 5, 1164 Sofia, Bulgaria

S. Trimper†
Fachbereich Physik, Martin-Luther-Universität, D-06099 Halle, Germany
(Received 4 September 2003; published 15 January 2004)

The origin of a central peak in the excitation spectra of thin ferroelectric films is ascribed to the relaxation of a surface mode. Contrary to the behavior in bulk materials the central peak appears even far from the phase-transition temperature, where it dominates the energy spectrum. The results are based on an Ising model in a transverse field. Applying a Green's-function formalism the complete transverse dynamic structure factor of ferroelectric thin films is calculated. That structure factor exhibits additional surface mode peaks, the occurrence of which gives rise to a central peak already at low temperatures. The results are in reasonable agreement with experimental data.

DOI: 10.1103/PhysRevB.69.024105 PACS number(s): 68.60.−p, 77.80.Bh

I. INTRODUCTION

Although surface and size effects on the behavior of ferroelectrics, in particular in the vicinity of a phase transition, had been discussed since the 1950s,[1] it aroused a renewed interest in that problem due to the rapid progress in the preparation and characterization of ferroelectric thin films and related composites. The influence of surface and size effects on the ferroelectric phase transitions had been extensively studied based on the Landau phenomenological theory.[2–4] Whereas Tilley and Zeks[4] studied in detail films which offer a second-order phase transition, Scott *et al.*[2] and Wang *et al.*[6] extended the analysis discussing first-order phase transitions. On the microscopic level, the pseudospin theory based on the Ising model in a transverse field (TIM) is a serious candidate to analyze the surface and size effects and their influence on the ferroelectric phase transitions. Cottam *et al.*[5] discussed the occurrence of surface modes in semi-infinite ferroelectrics, Wang *et al.*[6,7] and Sy[8] emphasized the role of the Curie temperature and its dependence on a change of the different model parameters.

The phase behavior of a thin ferroelectric film, described by the TIM, was recently investigated by Wang *et al.*[9,10] and by one of us.[11] The dynamical properties of thin films were explored within the random-phase approximation by Wang and Smith[12] however ignoring the effects of mode damping. The authors demonstrated that films, characterized by a reduced surface interaction in comparison with the bulk, exhibit a soft mode which corresponds to a surfacelike mode in the ferroelectric phase but to a bulklike mode in the paraelectric phase. In the opposite case of films with an enhanced surface interaction, the soft mode is a bulklike mode in the ferroelectric phase and a surfacelike mode in the paraelectric phase.

Klimpel and Dietrich[13] studied the neutron and x-ray scattering structure factor of thin films near to the critical point of the corresponding bulk system. Nkoma[14] developed a generalized theory of Raman scattering by bulk and surface polaritons in semi-infinite geometry. Using the Green's-function formalism Wesselinowa[15] calculated the temperature dependence of the soft modes of thin ferroelectric films based on the TIM including additionally damping effects. In particular, it was demonstrated in Ref. 15 that the soft-mode frequencies of thin ferroelectric films could be reduced, whereas the damping effects are enhanced compared to the bulk behavior.

The structure and dielectric properties of ferroelectric thin films had been studied using different experimental techniques, however, the lattice dynamics behavior related to ferroelectricity in thin films is not understood completely. Recently, several groups carried out Raman scattering measurements to characterize ferroelectric thin films. As the main result they found that all transverse-optical-phonon modes show a pronounced tendency to depart from their positions in the bulk single crystal, indicating that differences might exist between thin films and bulk single crystals.[16–21] Using Raman spectroscopy the temperature dependence of the phonon modes for thin ferroelectric films of $PbTiO_3$ is discussed by Taguchi *et al.*[19] and by Fu *et al.*[20] In contrast to the spectra in a single crystal, the Raman frequencies of ferroelectric thin films offer a significant shift to low frequencies and furthermore, the Raman lines are broadened. Moreover, the spectrum is dominated by a remarkable central-mode-type scattering pattern at all temperatures.[20] It seems that the intense quasielastic scattering in thin films can be attributed to a relaxation process described by a order-disorder transition. Such a mechanism is also the underlying one for the TIM. However, it is not clear at present why low-dimensional systems, such as thin films as well as ultrafine particles,[21] exhibit such a significant central-mode behavior at temperatures far from the phase transition. In view of the experimental findings it is interesting to examine the dynamic behavior of ferroelectric thin films in more detail. The aim of the present paper is to calculate the dynamic scattering function of thin ferroelectric films based on the TIM. In order to study the central peak in thin ferroelectric film we apply a Green's-function approach. Our results are consistent with experimental reports and in contrast to the bulk behavior observed in Refs. 22–24.

II. THE MODEL AND THE MATRIX GREEN'S FUNCTION

Let us first introduce the model and the corresponding matrix Green's function. We consider a three-dimensional ferroelectric system on a simple cubic lattice composed of N layers in z direction. The layers are numbered by $n=1,\ldots,N$, where the layers $n=1$ and $n=N$ represent the two surfaces of the system. The bulk is established by the other layers. To take into account specific surface effects we start with the Hamiltonian of the TIM including both, bulk and surface properties:

$$H=-\frac{1}{2}\sum_{ij} J_{ij}S_i^zS_j^z-\Omega_b\sum_{i\epsilon b} S_i^x-\Omega_s\sum_{i\epsilon s} S_i^x. \qquad (1)$$

Here S^x and S^z are the components of a spin-$\frac{1}{2}$ operator, and Ω_b and Ω_s represent the transverse fields in the bulk and in the different surface layers, respectively. The sum runs over the internal and the lattice points. Totally the system consists of N' lattice points. The parameter J_{ij} is an exchange interaction between spins at nearest-neighbor sites i and j. To take into account the effects originated by the finite thickness of the system, we introduce two interaction parameters J_b and J_s. In case of an interaction between spins, situated at the surface layer, the interaction strength is denoted by $J_{ij}=J_s$. Otherwise, the interaction in the bulk material is written as J_b, which is for simplicity assumed to be the same for the interlayer coupling between the surface layer and the bulk as well as the intralayer coupling between the different layers in the bulk. A similar notation is used for the transverse field Ω. The ordered phase is characterized by nonzero mean values $\langle S^x\rangle\neq 0$ and $\langle S^z\rangle\neq 0$. It is appropriate to introduce a new coordinate system by rotating the original one, used in Eq. (1), by an angle θ in the xz plane. The rotation angle θ is determined by the requirement $\langle S^{x'}\rangle=0$ in the new coordinate system.[25]

The retarded Green's function, to be calculated, is defined as

$$G_{ij}(t)=\langle\langle B_i(t);B_j^+(0)\rangle\rangle. \qquad (2)$$

The operator B_i stands symbolically for the set (S_i^+,S_i^-,S_i^z). Performing the two-dimensional Fourier transform, the Green's function $G_{n_in_j}(\mathbf{k}_\parallel,E)$ has the following form:

$$\langle\langle B_i^+;B_j^-\rangle\rangle_E=\frac{1}{N'}\sum_{\mathbf{k}_\parallel}\exp[i\mathbf{k}_\parallel(\mathbf{r}_i-\mathbf{r}_j)]G_{n_in_j}(\mathbf{k}_\parallel,E), \quad (3)$$

where N' is the total number of lattice sites in any of the lattice planes; $\mathbf{r}_i$ represents the position vectors at site i. As discussed above the number $n=1,\ldots,N$ characterizes the layer ordering beginning with $n=1$ (one surface) and terminating with the other surface $n=N$. The vector $\mathbf{k}_\parallel=(k_x,k_y)$ is a two-dimensional wave vector parallel to the surface. The summation is taken over the first Brillouin zone.

Now we calculate the Green's functions in an approximation, which goes beyond the random-phase approximation (RPA), for details we refer to Refs. 11 and 15. In that approach the coupling between the transverse and the longitudinal relaxing mode is taken into account. Furthermore, the Green's function reveals an imaginary part. Performing Fourier transformation we find that the Green's function for a ferroelectric thin film, defined by Eq. (3), obeys for $T\leqslant T_c$ the following $3N\times 3N$ matrix form:

$$\begin{pmatrix}\mathbf{H}_-(E) & -\mathbf{Q} & -\mathbf{P}\\ \mathbf{Q} & \mathbf{H}_+(E) & -\mathbf{P}\\ \mathbf{P} & \mathbf{P} & \mathbf{M}(E)\end{pmatrix}\begin{pmatrix}\mathbf{G}^{+-}\\ \mathbf{G}^{-+}\\ \mathbf{G}^{zz}\end{pmatrix}=\begin{pmatrix}\sigma\\ -\sigma\\ 0\end{pmatrix}. \quad (4)$$

In that equation the quantities $\mathbf{H},\mathbf{M},\mathbf{Q},\mathbf{P}$ are $N\times N$ matrices. $\mathbf{H}(E)$ is given by

$$\mathbf{H}_\mp=\begin{pmatrix}E\mp(v_1-i\gamma_1^{11}) & k_1 & 0 & 0 & 0 & 0 & \cdots\\ k_2 & E\mp(v_2-i\gamma_2^{11}) & k_2 & 0 & 0 & 0 & \cdots\\ 0 & k_3 & E\mp(v_3-i\gamma_3^{11}) & k_3 & 0 & 0 & \cdots\\ \vdots & \vdots & \vdots & \vdots & \vdots & \vdots & \ddots\\ 0 & 0 & 0 & 0 & 0 & k_N & E\mp(v_N-i\gamma_N^{11})\end{pmatrix} \quad (5)$$

with

$$k_n=J_b\sigma_n\sin^2\theta_n, \quad n=1,\ldots,N,$$

$$v_n=2\Omega_n\sin\theta_n+\frac{1}{2}\sigma_nJ_n\cos^2\theta_n-\frac{\sigma_nJ_n}{4}\sin^2\theta_n\gamma(\mathbf{k}_\parallel)+J_{n-1}\sigma_{n-1}\cos^2\theta_{n-1}+J_{n+1}\sigma_{n+1}\cos^2\theta_{n+1}$$
$$+\frac{J_n}{N\sigma_n}\sum_{\mathbf{q}_\parallel}\{0.5\sin^2\theta_n\gamma(\mathbf{q}_\parallel)\overline{m}_n(\mathbf{q}_\parallel)-[\gamma(\mathbf{q}_\parallel)\cos^2\theta_n-0.5\gamma(\mathbf{k}_\parallel-\mathbf{q}_\parallel)\sin^2\theta_n]\overline{n}_n(\mathbf{q}_\parallel)\}-\frac{J_{n-1}}{N\sigma_{n-1}}\sum_{\mathbf{q}_\parallel}\gamma(\mathbf{q}_\parallel)\cos^2\theta_{n-1}\overline{n}_{n-1}(\mathbf{q}_\parallel)$$
$$-\frac{J_{n+1}}{N\sigma_{n+1}}\sum_{\mathbf{q}_\parallel}\gamma(\mathbf{q}_\parallel)\cos^2\theta_{n+1}\overline{n}_{n+1}(\mathbf{q}_\parallel),$$

$$\gamma_n^{11}=\frac{\pi}{2N^2}\sum_{\mathbf{p}_\parallel,\mathbf{q}_\parallel}[[V_n(\mathbf{q}_\parallel,\mathbf{k}_\parallel-\mathbf{q}_\parallel)+V_n(\mathbf{k}_\parallel-\mathbf{p}_\parallel-\mathbf{q}_\parallel,\mathbf{p}_\parallel+\mathbf{q}_\parallel)]^2\{\bar{n}_n(\mathbf{p}_\parallel)[\sigma_n+\bar{n}_n(\mathbf{p}_\parallel+\mathbf{q}_\parallel)+\bar{n}_n(\mathbf{k}_\parallel-\mathbf{q}_\parallel)]-\bar{n}_n(\mathbf{p}_\parallel+\mathbf{q}_\parallel)\bar{n}_n(\mathbf{k}_\parallel-\mathbf{q}_\parallel)\}$$

$$\times\delta(\epsilon_n(\mathbf{k}_\parallel-\mathbf{q}_\parallel)+\epsilon_n(\mathbf{p}_\parallel+\mathbf{q}_\parallel)-\epsilon_n(\mathbf{p}_\parallel)-\epsilon_n(\mathbf{k}_\parallel))+\{[J_{n-1}\gamma(\mathbf{q}_\parallel)\cos^2\theta_{n-1}]^2+[J_{n-1}\gamma(\mathbf{k}_\parallel-\mathbf{p}_\parallel-\mathbf{q}_\parallel)\cos^2\theta_{n-1}]^2\}\{\bar{n}_{n-1}(\mathbf{p}_\parallel)$$

$$\times[\sigma_{n-1}+\bar{n}_{n-1}(\mathbf{p}_\parallel+\mathbf{q}_\parallel)+\bar{n}_{n-1}(\mathbf{k}_\parallel-\mathbf{q}_\parallel)]-\bar{n}_{n-1}(\mathbf{p}_\parallel+\mathbf{q}_\parallel)\bar{n}_{n-1}(\mathbf{k}_\parallel-\mathbf{q}_\parallel)\}\delta(\epsilon_{n-1}(\mathbf{k}_\parallel-\mathbf{q}_\parallel)+\epsilon_{n-1}(\mathbf{p}_\parallel+\mathbf{q}_\parallel)-\epsilon_{n-1}(\mathbf{p}_\parallel)$$

$$-\epsilon_{n-1}(\mathbf{k}_\parallel))+\{[J_{n+1}\gamma(\mathbf{q}_\parallel)\cos^2\theta_{n+1}]^2+[J_{n+1}\gamma(\mathbf{k}_\parallel-\mathbf{p}_\parallel-\mathbf{q}_\parallel)\cos^2\theta_{n+1}]^2\}\{\bar{n}_{n+1}(\mathbf{p}_\parallel)[\sigma_{n+1}+\bar{n}_{n+1}(\mathbf{p}_\parallel+\mathbf{q}_\parallel)+\bar{n}_{n+1}(\mathbf{k}_\parallel$$

$$-\mathbf{q}_\parallel)]-\bar{n}_{n+1}(\mathbf{p}_\parallel+\mathbf{q}_\parallel)\bar{n}_{n+1}(\mathbf{k}_\parallel-\mathbf{q}_\parallel)\}\delta(\epsilon_{n+1}(\mathbf{k}_\parallel-\mathbf{q}_\parallel)+\epsilon_{n+1}(\mathbf{p}_\parallel+\mathbf{q}_\parallel)-\epsilon_{n+1}(\mathbf{p}_\parallel)-\epsilon_{n+1}(\mathbf{k}_\parallel))-\sin^2\theta_n V_n(\mathbf{q}_\parallel,\mathbf{k}_\parallel-\mathbf{q}_\parallel)$$

$$\times\{J_b[\gamma(\mathbf{p}_\parallel)+\gamma(\mathbf{p}_\parallel+\mathbf{q}_\parallel)]\bar{m}_n(\mathbf{p}_\parallel+\mathbf{q}_\parallel)[\bar{n}_n(\mathbf{p}_\parallel)-\bar{n}_n(\mathbf{k}_\parallel-\mathbf{q}_\parallel)]+J_b[\gamma(\mathbf{p}_\parallel)+\gamma(\mathbf{k}_\parallel-\mathbf{q}_\parallel)]\bar{m}_n(\mathbf{k}_\parallel-\mathbf{q}_\parallel)[\bar{n}_n(\mathbf{p}_\parallel)-\bar{n}_n(\mathbf{p}_\parallel+\mathbf{q}_\parallel)]\}$$

$$\times\delta(\epsilon_n(\mathbf{k}_\parallel-\mathbf{q}_\parallel)+\epsilon_n(\mathbf{p}_\parallel+\mathbf{q}_\parallel)-\epsilon_n(\mathbf{p}_\parallel)-\epsilon_n(\mathbf{k}_\parallel))-\sin^2\theta_{n-1}[J_{n-1}\gamma(\mathbf{q}_\parallel)\cos^2\theta_{n-1}+J_{n-1}\gamma(\mathbf{k}_\parallel-\mathbf{p}_\parallel-\mathbf{q}_\parallel)\cos^2\theta_{n-1}]$$

$$\times\{J_b[\gamma(\mathbf{p}_\parallel)+\gamma(\mathbf{p}_\parallel+\mathbf{q}_\parallel)]\bar{m}_{n-1}(\mathbf{p}_\parallel+\mathbf{q}_\parallel)[\bar{n}_{n-1}(\mathbf{p}_\parallel)-\bar{n}_{n-1}(\mathbf{k}_\parallel-\mathbf{q}_\parallel)]+J_b[\gamma(\mathbf{p}_\parallel)+\gamma(\mathbf{k}_\parallel-\mathbf{q}_\parallel)]\bar{m}_{n-1}(\mathbf{k}_\parallel-\mathbf{q}_\parallel)[\bar{n}_{n-1}(\mathbf{p}_\parallel)$$

$$-\bar{n}_{n-1}(\mathbf{p}_\parallel+\mathbf{q}_\parallel)]\}\delta(\epsilon_{n-1}(\mathbf{k}_\parallel-\mathbf{q}_\parallel)+\epsilon_{n-1}(\mathbf{p}_\parallel+\mathbf{q}_\parallel)-\epsilon_{n-1}(\mathbf{p}_\parallel)-\epsilon_{n-1}(\mathbf{k}_\parallel))-\sin^2\theta_{n+1}[J_{n+1}\gamma(\mathbf{q}_\parallel)\cos^2\theta_{n+1}+J_{n+1}\gamma(\mathbf{k}_\parallel$$

$$-\mathbf{p}_\parallel-\mathbf{q}_\parallel)\cos^2\theta_{n+1}]\{J_b[\gamma(\mathbf{p}_\parallel)+\gamma(\mathbf{p}_\parallel+\mathbf{q}_\parallel)]\bar{m}_{n+1}(\mathbf{p}_\parallel+\mathbf{q}_\parallel)[\bar{n}_{n+1}(\mathbf{p}_\parallel)-\bar{n}_{n+1}(\mathbf{k}_\parallel-\mathbf{q}_\parallel)]+J_b[\gamma(\mathbf{p}_\parallel)+\gamma(\mathbf{k}_\parallel-\mathbf{q}_\parallel)]$$

$$\times\bar{m}_{n+1}(\mathbf{k}_\parallel-\mathbf{q}_\parallel)[\bar{n}_{n+1}(\mathbf{p}_\parallel)-\bar{n}_{n+1}(\mathbf{p}_\parallel+\mathbf{q}_\parallel)]\}\delta(\epsilon_{n+1}(\mathbf{k}_\parallel-\mathbf{q}_\parallel)+\epsilon_{n+1}(\mathbf{p}_\parallel+\mathbf{q}_\parallel)-\epsilon_{n+1}(\mathbf{p}_\parallel)-\epsilon_{n+1}(\mathbf{k}_\parallel))],$$

$$\gamma(\mathbf{k}_\parallel)=\tfrac{1}{2}[\cos(k_x a)+\cos(k_y a)],$$

$$\bar{n}_n(\mathbf{q}_\parallel)=\frac{\sigma_n}{2}\left[\frac{J_n\sigma_n}{2\epsilon_n(\mathbf{q}_\parallel)}\left(1-0.5\sin^2\theta_n\gamma(\mathbf{q}_\parallel)\coth\frac{\epsilon_n(\mathbf{q}_\parallel)}{2T}-1\right)\right.,$$

$$\bar{m}_n(\mathbf{q}_\parallel)=\frac{\sigma_n^2}{8\epsilon_n(\mathbf{q}_\parallel)}\sin^2\theta_n J_n\gamma(\mathbf{q}_\parallel)\coth\frac{\epsilon_n(\mathbf{q}_\parallel)}{2T},$$

$$V_n(\mathbf{q}_\parallel,\mathbf{k}_\parallel-\mathbf{q}_\parallel)=J_n[\cos^2\theta_n\gamma(\mathbf{q}_\parallel)-0.5\sin^2\theta_n\gamma(\mathbf{k}_\parallel-\mathbf{q}_\parallel)].$$

Here $\epsilon_n(\mathbf{k}_\parallel)$ is the transverse pseudospin energy of the nth layer, which is related to the poles of the transverse Green's function. The quantity $\gamma_n^{11}(\mathbf{k}_\parallel)$ is the transverse spin-wave damping of the nth layer. Here we have used the notations, introduced above: $J_1=J_N=J_s$, $J_n=J_b$ $(n=2,3,4,\ldots,N-1)$, $\Omega_1=\Omega_N=\Omega_s$, $\Omega_n=\Omega_b$ $(n=2,3,4,\ldots,N-1)$, $J_0=J_{N+1}=0$. $\sigma(T)$ is the relative polarization in the direction of the mean field and is equal to $2\langle S^{z'}\rangle$. The matrix $\mathbf{Q}$ is given by the following expression:

$$\mathbf{Q}=\begin{pmatrix} d_1 & k_1 & 0 & 0 & 0 & 0 & \cdots \\ k_2 & d_2 & k_2 & 0 & 0 & 0 & \cdots \\ 0 & k_3 & d_3 & k_3 & 0 & 0 & \cdots \\ \vdots & \vdots & \vdots & \vdots & \vdots & \vdots & \ddots \\ 0 & 0 & 0 & 0 & 0 & k_N & d_N \end{pmatrix} \tag{6}$$

with

$$k_n=J_b\sigma_n\sin^2\theta_n, \quad n=1,\ldots,N,$$

$$d_n=-\frac{\sigma_n J_n}{4}\sin^2\theta_n\gamma(\mathbf{k}_\parallel).$$

The matrix $\mathbf{P}$ reads

$$\mathbf{P}=\begin{pmatrix} t_1 & l_1 & 0 & 0 & 0 & 0 & \cdots \\ l_2 & t_2 & l_2 & 0 & 0 & 0 & \cdots \\ 0 & l_3 & t_3 & l_3 & 0 & 0 & \cdots \\ \vdots & \vdots & \vdots & \vdots & \vdots & \vdots & \ddots \\ 0 & 0 & 0 & 0 & 0 & l_N & t_N \end{pmatrix} \tag{7}$$

with

$$l_n=\frac{1}{2N'}\sin^2\theta_n J_n\sum_{\mathbf{q}_\parallel}\gamma(\mathbf{k}_\parallel-\mathbf{q}_\parallel)(\langle S_{\mathbf{q}_\parallel}^+S_{-\mathbf{q}_\parallel}^z\rangle_n-\langle S_{\mathbf{q}_\parallel}^-S_{\mathbf{q}_\parallel}^z\rangle_n),$$

$$t_n=\frac{1}{2N'}\sin^2\theta_n J_n\sum_{\mathbf{q}_\parallel}(\langle S_{\mathbf{q}_\parallel}^+S_{-\mathbf{q}_\parallel}^z\rangle_n-\langle S_{\mathbf{q}_\parallel}^-S_{\mathbf{q}_\parallel}^z\rangle_n),$$

and the matrix $\mathbf{M}$, included in Eq. (4), is

$$\mathbf{M}=\begin{pmatrix} E-i\gamma_1^{33} & l_1 & 0 & 0 & 0 & 0 & \cdots \\ l_2 & E-i\gamma_2^{33} & l_2 & 0 & 0 & 0 & \cdots \\ 0 & l_3 & E-i\gamma_3^{33} & l_3 & 0 & 0 & \cdots \\ \vdots & \vdots & \vdots & \vdots & \vdots & \vdots & \ddots \\ 0 & 0 & 0 & 0 & 0 & l_N & E-i\gamma_N^{33} \end{pmatrix} \tag{8}$$

with

$$l_n=\frac{1}{2N'}\sin^2\theta_n J_n\sum_{\mathbf{q}_\parallel}\gamma(\mathbf{k}_\parallel-\mathbf{q}_\parallel)(\langle S^+_{\mathbf{q}_\parallel}S^z_{-\mathbf{q}_\parallel}\rangle_n-\langle S^-_{\mathbf{q}_\parallel}S^z_{\mathbf{q}_\parallel}\rangle_n),$$

$$\begin{aligned}\gamma_n^{33}=\frac{\pi}{16N'}\sum_{\mathbf{q}_\parallel}&[\sin^4\theta_n[J_n\gamma(\mathbf{q}_\parallel)+J_n\gamma(\mathbf{k}_\parallel-\mathbf{q}_\parallel)]^2[\sigma_n+\overline{n}_n(\mathbf{q}_\parallel)+\overline{n}_n(\mathbf{k}_\parallel-\mathbf{q}_\parallel)]\delta(\epsilon_n(\mathbf{q}_\parallel)+\epsilon_n(\mathbf{k}_\parallel-\mathbf{q}_\parallel)-\epsilon_n(\mathbf{k}_\parallel))\\
&+\sin^4\theta_n[J_n\gamma(\mathbf{q}_\parallel)-J_n\gamma(\mathbf{k}_\parallel-\mathbf{q}_\parallel)]^2[\overline{n}_n(\mathbf{q}_\parallel)-\overline{n}_n(\mathbf{k}_\parallel-\mathbf{q}_\parallel)][\delta(\epsilon_n(\mathbf{k}_\parallel-\mathbf{q}_\parallel)-\epsilon_n(\mathbf{q}_\parallel)-\epsilon_n(\mathbf{k}_\parallel))-\delta(\epsilon_n(\mathbf{q}_\parallel)-\epsilon_n(\mathbf{k}_\parallel-\mathbf{q}_\parallel)\\
&-\epsilon_n(\mathbf{k}_\parallel))]+\sin^4\theta_{n-1}[J_{n-1}\gamma(\mathbf{q}_\parallel)+J_{n-1}\gamma(\mathbf{k}_\parallel-\mathbf{q}_\parallel)]^2[\sigma_n+\overline{n}_{n-1}(\mathbf{q}_\parallel)+\overline{n}_{n-1}(\mathbf{k}_\parallel-\mathbf{q}_\parallel)]\delta(\epsilon_{n-1}(\mathbf{q}_\parallel)+\epsilon_{n-1}(\mathbf{k}_\parallel-\mathbf{q}_\parallel)\\
&-\epsilon_{n-1}(\mathbf{k}_\parallel))+\sin^4\theta_{n-1}[J_{n-1}\gamma(\mathbf{q}_\parallel)-J_{n-1}\gamma(\mathbf{k}_\parallel-\mathbf{q}_\parallel)]^2[\overline{n}_{n-1}(\mathbf{q}_\parallel)-\overline{n}_{n-1}(\mathbf{k}_\parallel-\mathbf{q}_\parallel)][\delta(\epsilon_{n-1}(\mathbf{k}_\parallel-\mathbf{q}_\parallel)-\epsilon_{n-1}(\mathbf{q}_\parallel)\\
&-\epsilon_{n-1}(\mathbf{k}_\parallel))-\delta(\epsilon_{n-1}(\mathbf{q}_\parallel)-\epsilon_{n-1}(\mathbf{k}_\parallel-\mathbf{q}_\parallel)-\epsilon_{n-1}(\mathbf{k}_\parallel))]+\sin^4\theta_{n+1}[J_{n+1}\gamma(\mathbf{q}_\parallel)+J_{n+1}\gamma(\mathbf{k}_\parallel-\mathbf{q}_\parallel)]^2[\sigma_n+\overline{n}_{n+1}(\mathbf{q}_\parallel)\\
&+\overline{n}_{n+1}(\mathbf{k}_\parallel-\mathbf{q}_\parallel)]\delta(\epsilon_{n+1}(\mathbf{q}_\parallel)+\epsilon_{n+1}(\mathbf{k}_\parallel-\mathbf{q}_\parallel)-\epsilon_{n+1}(\mathbf{k}_\parallel))+\sin^4\theta_{n+1}[J_{n+1}\gamma(\mathbf{q}_\parallel)-J_{n+1}\gamma(\mathbf{k}_\parallel-\mathbf{q}_\parallel)]^2[\overline{n}_{n+1}(\mathbf{q}_\parallel)\\
&-\overline{n}_{n+1}(\mathbf{k}_\parallel-\mathbf{q}_\parallel)][\delta(\epsilon_{n+1}(\mathbf{k}_\parallel-\mathbf{q}_\parallel)-\epsilon_{n+1}(\mathbf{q}_\parallel)-\epsilon_{n+1}(\mathbf{k}_\parallel))-\delta(\epsilon_{n+1}(\mathbf{q}_\parallel)-\epsilon_{n+1}(\mathbf{k}_\parallel-\mathbf{q}_\parallel)-\epsilon_{n+1}(\mathbf{k}_\parallel))]].\end{aligned}$$

III. THE TRANSVERSE DYNAMIC STRUCTURE FACTOR

In this section we present the transverse dynamic structure factor $S^{xx}(\mathbf{k}_\parallel,E)$ which is obtained via the imaginary part of the matrix Green's function $G(\mathbf{k}_\parallel,E)$ after inversion of Eq. (4). To perform this calculation, as already stressed above, one has to go beyond the conventional RPA which provides an imaginary part, i.e., damping effects are incorporated. For $S^{xx}(\mathbf{k}_\parallel,E)$ we get

$$S^{xx}(\mathbf{k}_\parallel,E)=\frac{4\sigma(\epsilon^{11}_{\mathbf{k}}-\epsilon^{12}_{\mathbf{k}})}{(1-e^{-E/T})}\frac{\mathrm{Re}\Gamma^{xx}_{\mathbf{k}}(E)}{[E^2-\epsilon^2_{\mathbf{k}}-\mathrm{Im}\Gamma^{xx}_{\mathbf{k}}(E)]^2+[\mathrm{Re}\Gamma^{xx}_{\mathbf{k}}(E)]^2}. \tag{9}$$

$\mathrm{Re}\Gamma^{xx}_{\mathbf{k}}(E)$ and $\mathrm{Im}\Gamma^{xx}_{\mathbf{k}}(E)$ are the real and the imaginary parts of $\Gamma^{xx}_{\mathbf{k}}(E)$ which are related to the matrix elements of **H**, **Q**, **P**, and **M**. The quantities ϵ^{11}, ϵ^{12}, ϵ^{13} are obtained from the matrices **H**, **Q**, **P**, defined in Eqs. (5)–(7), and $\epsilon_{\mathbf{k}}=\sqrt{(\epsilon^{11})^2-(\epsilon^{12})^2}$. The quantity

$$\Gamma^{xx}_{\mathbf{k}}(E)=2E(\gamma^{11}_s+\gamma^{11}_b)+\frac{i2(\epsilon^{13}_s+\epsilon^{13}_b)^2E}{E+i(\gamma^{33}_s+\gamma^{33}_b)} \tag{10}$$

describes the coupling of the transverse soft mode to a longitudinal relaxation mode.[24] It is eventually responsible for the occurrence of the central peak which is discussed below.

In case of an infinite ferroelectric crystal a central peak appears in the ferroelectric region at the energy $E=0$ together with two soft-mode peaks with an energy $E=\pm\omega_{\mathrm{soft}}=\pm\sqrt{\epsilon^2_{\mathbf{k}}+\epsilon^2_{13}}$ as depicted in Fig. 1. At low temperatures the structure factor S^{xx} reveals only the sharp soft-mode peak. With increasing temperature T the soft mode peak becomes lower and broader and is shifted towards the origin. In the vicinity of the phase-transition temperature T_c a central peak appears additionally to the soft-mode peak. A relaxing mode,

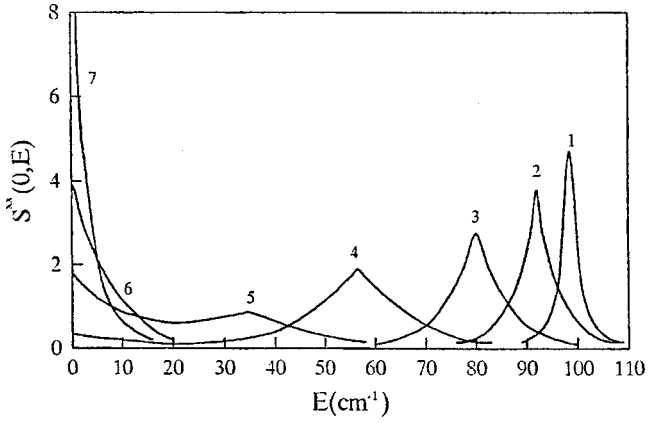

FIG. 1. Transverse dynamic structure factor $S^{xx}(\mathbf{k}_\parallel,E)$ for an infinite ferroelectric KDP crystal [$J_b=495$ K, $\Omega_b=124$ K, $T_c=123$ K (Ref. 26)] as a function of the energy E for $\mathbf{k}=0$ and for different temperatures: 1, $T=20$, 2, 40; 3, 60; 4, 100; 5, 115; 6, 120; 7, 122 K.

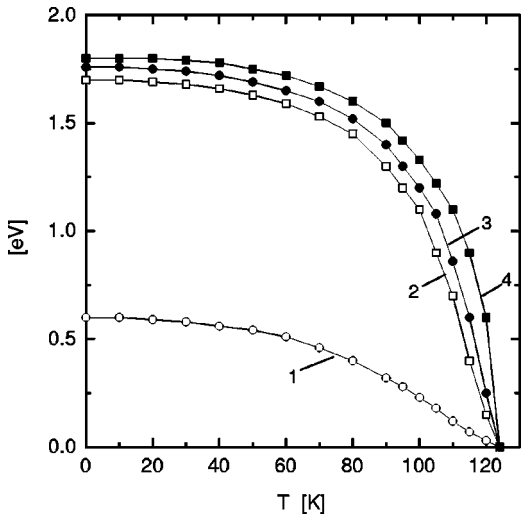

FIG. 2. Temperature dependence of the excitation spectra for thin ($N=8$ layers) ferroelectric KDP film for $\mathbf{k}=0$, $J_s=2J_b$, $\Omega_s=0.2\Omega_b$ for different layers: 1, $n=1;2$, $n=2;3$, $n=3;4$, $n=4$.

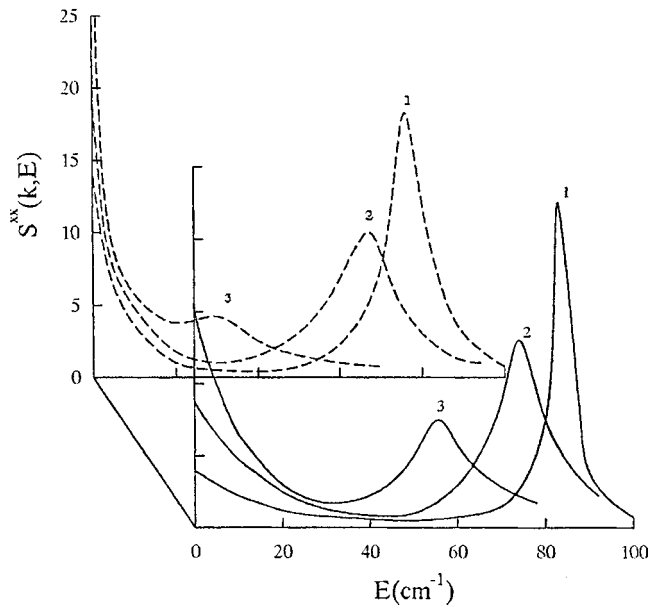

FIG. 3. Transverse dynamic structure factor $S^{xx}(\mathbf{k}_\parallel,E)$ for a thin ($N=8$ layers) ferroelectric KDP film as a function of the energy E for $\mathbf{k}=0$, $J_s=1.2J_b$, $\Omega_s=0.2\Omega_b$ (full line) and $J_s=2.0J_b$, $\Omega_s=0.2\Omega_b$ (dashed line), and for different temperatures: 1, $T=20$; 2, 50; 3, 100 K.

associated with the central peak, appears below the soft-mode line when the phase transition is approached. Near to T_c the intensity of the soft mode peak is strongly reduced whereas the intensity of the central peak is enhanced drastically. Thus, the soft-mode is underdamped at low temperatures and overdamped near and above T_c. The additional longitudinal mode becomes purely imaginary, $E_{33}=-i\gamma_{33}$.

Now let us discuss the temperature dependence of the modes obtained for a ferroelectric thin film. Obviously, the behavior of such material is strongly influenced by the parameters of the surface. In particular, the critical properties are highly sensitive to those parameters. They dominate the behavior of thin films at low temperatures more than in the bulk. The surface energy is much smaller than the energy of an inner layer. This can be ascribed to the lower coordination number of a spin at the surface. In Fig. 2 the temperature dependence of the excitation spectra $\epsilon_{\mathbf{k}}$ is presented. The surface mode is clearly distinguished (curve 1) from the bulk modes (curves 2, 3, and 4). With increasing J_s the difference between the surface and the bulk modes is enhanced. Furthermore, the damping of surface modes is much higher compared to those modes observed at an inner layer. The considerable difference between the surface spectrum and the spectrum of the inner layer can be traced back to the occurrence of additional surface modes, the damping of which increases rapidly by crossing over into the bulk. The spin-wave frequencies of thin ferroelectric films are smaller, whereas the damping effects are larger in comparison to the bulk.[15] The result is also in agreement with the experimental data which had been demonstrated in a series of different investigations.[17,19,20] In our case this observation means, that for all temperatures, the transverse damping fulfills the relation $\gamma_s^{11}>\gamma_b^{11}$ whereas the damping of the longitudinal modes satisfies $\gamma_s^{33}>\gamma_b^{33}$. As stressed already above, the origin of the central peak at low temperatures is different from that in the bulk case. It is related to the existence of a surface mode. The width of the central peak, Γ_c, is obtained from the imaginary part of the quantity Γ, given in Eq. (10). The width is proportional to the longitudinal damping:

$$\Gamma_c=(\gamma_s^{33}+\gamma_b^{33})\frac{\epsilon_{\mathbf{k}}^2}{(\omega_s^2+\omega_b^2)_{\text{soft}}}. \tag{11}$$

The relaxation mechanism of the surface mode sets in before the relaxing mechanism of the bulk mode. The surface of the thin film can be overdamped already at low temperatures, whereas the soft mode of the bulk is overdamped mainly near T_c. Therefore, the transverse dynamic structure factor S^{xx} exhibits yet for low temperatures a central peak at zero energy $E=0$ which is drawn in Fig. 3. The curves are in agreement with the experimental data obtained by Fu *et al.*[20] Whereas for thin films the central peak appears already for $T=20$ K, see curve 1 in Fig. 3, in the bulk material such behavior is observed first at $T=100$ K as depicted in Fig. 1 (curve 4). The origin of the different behavior is attributed to the occurrence of a surface mode. The intensity of the central peak at low temperatures increases with decreasing film thickness and with increasing two-spin interaction constant J_s. Simultaneously, the intensity of the sideband peaks decreases with decreasing film thickness.

The picture of the dynamic structure factor $S^{xx}(\mathbf{k}_\parallel,E)$ of thin ferroelectric films is obtained by a superposition of two peaks. At low temperatures there are two sideband soft-mode peaks, which originate mainly in the bulk modes and furthermore there is a central peak due to the surface soft modes. The sideband soft-mode peaks are shifted to lower frequencies and are broader compared to those of the bulk. This result is caused by the interaction of surface and bulk modes. Approaching T_c the sideband soft-mode peaks are shifted to

the origin and contribute to the central peak, i.e., near T_c there is a central peak, generated by both the surface and the bulk modes. Note that the central peak in case of bulk material occurs only in the vicinity of the critical temperature.

IV. CONCLUSIONS

In conclusions, a Green's-function formalism is used to calculate the dynamic structure factor of thin ferroelectric films based on the Ising model in a transverse field. We have shown that the spectrum consists of a remarkable central mode at temperatures far from the phase transition in contrast to the case of the bulk. The central peak at low temperatures disappears when the thickness of the film increases. Moreover, the intensity of the central peak increases with increasing the surface spin-spin-interaction constant J_s, i.e., the central peak is caused predominantly by the surface modes. This is a possible mechanism to explain the central peak observed in the excitation spectra of ferroelectric thin films. The results are in agreement with experimental findings.

It will be of interest to investigate the influence of the other interaction constants—tunneling frequency, four-spin-interaction constant—of the surface and of the bulk on the position, intensity, and width of the peaks. The interaction between the pseudospins and the phonons should also be taken into account.[23,24] This will be published elsewhere.

ACKNOWLEDGMENTS

One of us (J.M.W.) is grateful to the Deutsche Forschungsgemeinschaft for financial support. This work was supported by Grant No. SFB 418.

*Electronic address: julia@phys.uni-sofia.bg
†Electronic address: trimper@physik.uni-halle.de

[1] J. Jacard, W. Kanzig, and M. Peter, Helv. Phys. Acta **26**, 521 (1953).
[2] J.F. Scott, H.M. Duiker, P.D. Belae, B. Pouligny, K. Dimmler, M. Darris, D. Butler, and S. Eaton, Physica B **150**, 160 (1988).
[3] K. Binder, Ferroelectrics **35**, 99 (1987).
[4] D.R. Tilley and B. Zeks, Solid State Commun. **49**, 823 (1984).
[5] M.G. Cottam, D.R. Tilley, and B. Zeks, J. Phys. C **17**, 1793 (1984).
[6] Y.G. Wang, W.L. Zhong, and P.L. Zhang, Phys. Rev. B **53**, 11 439 (1996).
[7] C.L. Wang, W.L. Zhong, and P.L. Zhang, J. Phys.: Condens. Matter **3**, 4743 (1992).
[8] H.K. Sy, J. Phys.: Condens. Matter **5**, 1213 (1993).
[9] C.L. Wang, S.R.P. Smith, and D.R. Tilley, J. Phys.: Condens. Matter **6**, 9633 (1994).
[10] X.G. Wang, S.H. Pan, and G.Z. Yang, J. Phys.: Condens. Matter **11**, 6581 (1999).
[11] J.M. Wesselinowa, Phys. Status Solidi B **223**, 737 (2001).
[12] C.L. Wang and S.R.P. Smith, J. Phys.: Condens. Matter **8**, 3075 (1996).
[13] R. Klimpel and S. Dietrich, Phys. Rev. B **60**, 16 977 (1999).
[14] J.S. Nkoma, J. Phys.: Condens. Matter **11**, 4093 (1999).
[15] J.M. Wesselinowa, Phys. Status Solidi B **231**, 187 (2002).
[16] Z.C. Feng, B.S. Kwak, A. Erbil, and L.A. Boatner, Appl. Phys. Lett. **62**, 349 (1993).
[17] E. Ching-Prado, A. Reynes-Figueroa, R.S. Katiyar, S.B. Majumder, and D.C. Agrawal, J. Appl. Phys. **78**, 1920 (1995).
[18] L. Sun, Y.F. Chen, L. He, C.Z. Ge, D.S. Ding, T. Yu, M.S. Zhang, and N.B. Ming, Phys. Rev. B **55**, 12 218 (1997).
[19] I. Taguchi, A. Pignolet, L. Wang, M. Proctor, F. Levy, and P.E. Schmid, J. Appl. Phys. **73**, 394 (1993).
[20] D.S. Fu, H. Iwazaki, H. Suzuki, and K. Ishikawa, J. Phys.: Condens. Matter **12**, 399 (2000).
[21] K. Ishikawa, K. Yoshikawa, and N. Okada, Phys. Rev. B **37**, 5852 (1988).
[22] M.D. Fontana, H. Idrissi, G.E. Kugel, and K. Wojicik, J. Phys.: Condens. Matter **3**, 8695 (1991).
[23] J.M. Wesselinowa, Phys. Rev. B **49**, 3098 (1994).
[24] J.M. Wesselinowa and A.T. Apostolov, Solid State Commun. **101**, 343 (1997); Phys. Status Solidi B **201**, 529 (1997).
[25] W. Haubenreisser, W. Brodkorb, A. Corciovei, and G. Costache, Phys. Status Solidi B **53**, 9 (1992).
[26] P. Peercy, Phys. Rev. B **9**, 4868 (1974).